Neutronic studies of an irradiation facility coupled to a proton cyclotron

João Pedro Oliveira Lourenço

Instituto Superior Técnico, Lisboa, Portugal

June 2019

Abstract

This work investigated if, and how, it is viable to use a 250 MeV proton cyclotron for radiation therapy, foreseen to be installed in CTN, IST, coupled to a target, to produce a neutron beam. Using the Monte-Carlo simulation code MCNPX a target was selected and dimensioned, which was done by simulating a 250 MeV proton beam incident in several targets and analysing the neutron beam thus produced. To provide irradiation positions with thermal and fast neutrons, two configurations were studied. The materials and dimensions of the components of the irradiation apparatus, for both configurations, were characterized and optimized and the fast and thermal irradiation positions of these configurations were compared, using the neutron ratios and spectra at those positions. The radiation dose rates, in the vicinity of the irradiation apparatus, were investigated and a biological shield surrounding it was implemented to guarantee that the radiation protection safety norms are fulfilled. Using CINDER'90 code, the activation of the target and the components of the irradiation apparatus was also calculated.

Keywords: Cyclotron, Neutron sources, Radiation shielding, Monte-Carlo, Neutron activation

1. Introduction

Neutrons of a wide range of energies and intensities are useful in a variety of applications, from basic research to medical treatment. In this work the use of a cyclotron coupled to a target for the production of neutrons for research applications is going to be studied. The installation, in the near future, of a 250 MeV proton cyclotron for radiation therapy is foreseen in the Loures Campus of IST [2]. Therefore, in this work, this cyclotron was considered as a source of protons for irradiation of a neutron producing target. To study the viability of producing neutrons with a 250 MeV cyclotron, this work was divided in three stages: (i) investigating the yield of neutrons obtained from the nuclear reactions of the proton beam in several targets, in order to chose the best one; (ii) planning an irradiation position with a spectrum rich in fast neutrons ($E > 1$ MeV) and an irradiation position with a spectrum rich in thermal neutrons ($E < 0.5$ eV); (iii) characterizing the shielding of the irradiation apparatus for neutrons and γ, in addition to simulate the activation of the materials used in the irradiation apparatus, due to the nuclear reactions that occur in its different components.

2. Methodology

The Monte-Carlo simulation code used through out this work was MCNPX [10]. Its data base contains experimental cross sections for (p, n) reactions for most of the elements. However, when there is no experimental data for certain isotopes, it uses the results from Bertini's theoretical model [5, 6]. Bertini's model is based on a nucleon-nucleus interaction proposed by Serber [11]. It assumes two different interaction regimes: initially the incident nucleon initiates a cascade of interactions individually with each nucleon, inside the target nucleus, with cross sections slightly modified from the ones between free particles to account for the Pauli exclusion principle. In the second regime (corresponding to lower energy), the compound nucleus will de-excite through a mechanism called "evaporation" characterized by a slow loss of energy, due to the multiple scattering of the nucleons inside the compound nucleus.

In MCNPX the estimate of the expected value of a quantity (for example, the number of particles) is called tally and, unless otherwise specified in the MCNPX input file, the results are normalized to one source particle. In this work, three different tally types were used: (i) f1 type tally - counts the number of particles of a given type (protons, electrons, neutrons, ...) crossing a specified surface; (ii) f2 type tally - average fluence (in $\frac{\text{\# of particles}}{cm^2}$) across a specified surface, of a given particle type; (iii) f4 type tally - average fluence (in

$\frac{\text{\# of particles}}{cm^2}$) across the surfaces of a particular volume (in MCNPX called a cell), of a given particle type. In this work two tally modification commands, also known as cards, are going to be used: (i) FM card - multiplying a tally output by some quantity; (ii) DF card - multiplying a tally output by a fluence-to-dose conversion factor.

CINDER'90 is another simulation code [14], which was used for calculating the activity and radionuclides produced in the components of the irradiation apparatus. It is coupled to a nuclear data library, that provides the inventory of nuclides in an irradiated material, by calculating the atom density and activity density of every nuclide at a specific time. In this work, this code is used to describe the activation of the irradiation apparatus. To calculate the atom density of a nuclide, the Bateman equations must be solved. They give the rate of change of the atom density of nuclide m ($\dot{N}_m(t)$), which is obtained by summing the rates of losses and gains of the nuclide density. In some cases, an additional constant production rate for nuclide m ($\bar{Y}_m$) can be included and so, the differential equation for the rate of change of the atom density of nuclide m can be written has [14]:

$$\dot{N}_m(t) = -N_m(t)\beta_m + \bar{Y}_m + \sum_{k \neq m} N_k(t)\gamma_{k \to m} \, , \quad (1)$$

where $\beta_m = \lambda_m + \phi\sigma_m^a$ (ϕ is the neutron fluence integrated in energy, λ_m is the total decay constant of nuclide m and σ_a^m is the fluence-weighted average cross section for neutron absorption of nuclide m) and $\gamma_{k \to m}$ is the probability of a nuclide k to transmute, by radioactive-decay or particle absorption, to nuclide m.

Even though the Bateman equations (1) are coupled, they can be reduced to a set of more convenient independent equations by using the Markovian property: the probability of decay is independent of time and is equal for all nuclei of a given species, independently of how they were formed:

$$\dot{N}_i(t) = \bar{Y}_i + N_{i-1}(t)\gamma_{i-1} - N_i(t)\beta_i \, , \quad (2)$$

where the rate of change of the (partial) atom density of the i_{th} element of the linear chain, $N_i(t)$, is only coupled to the preceding element in the sequence. This means that the partial atom density of each nuclide only depends on itself and on the previous nuclide in the linearised chain. The total atom densities are obtained by solving for the partial concentrations of each nuclide in every linear chain and then by summing these partial concentrations to get the total atom densities.

3. Target selection

The study of the design of the irradiation apparatus (system cyclotron plus target) begins by surveying different target materials in order to choose the best candidate for producing a neutron beam with the required characteristics for this work. Since it was not clear whether the best target is made from a low- or a high-mass number material, the materials chosen to be surveyed were Aluminium, Beryllium and Carbon for the light targets, and Bismuth, Lead, Tantalum and Tungsten for the heavy targets. In order to chose from these candidates, several aspects were compared: the transmitted neutron spectra and beam purity (neutrons per proton ratio), at the end of each target, are the most important but the toxicity, activation and thermal properties of the materials were also taken in account.

3.1. Dimensioning the targets

As a result of the collisions of the protons in the target material, there will be a significant broadening of the proton beam. So, if the cross-section area of the target is too low, there will be leakage of protons through its side walls and, to reduce it, a suitable cross-section area for each target must be found. To define the cross-section area of the targets, the number of protons per source proton (f1 type tally) that leak through their side walls must be calculated, giving a rough estimate of the cross-section area that is needed to mitigate this leakage. The number of leaked protons were calculated at only one of the four side walls of the targets because, since the proton beam has Y-Z symmetry around the initial beam direction (X axis), the same leakage occurs in every side wall.

In this work, if the number of leaked protons is lower than 5E−6 protons/source proton, it was considered that the cross-section areas of the targets are sufficiently large. After establishing the cross-section areas of the targets, their optimal thickness must be set. Since the objective of the irradiation apparatus is to produce a neutron beam, it is desirable to maximize the transmitted neutrons, leaving the targets, while minimizing the transmitted protons. Therefore, the transmitted neutrons per proton ratio, taken at the end of the targets, must be maximized. The thicknesses that maximize the transmitted neutrons/proton ratio is presented in table 1. In this table it can be seen that the transmitted neutrons/proton ratio is lower on light targets (Al, Be and C) than on heavy targets (Bi, Pb, Ta and W). Besides, it was also found that the transmitted number of neutrons are lower on light targets than on heavy targets. This means that a heavy target must be used in this work, since it produces a more pure and intense neutron beam.

Materials	Thickness (cm)	Neutrons/Proton
W	4.0	1.96E+03
Ta	4.6	2.08E+03
Pb	7.1	2.26E+03
Bi	8.1	1.82E+03
Al	19.0	2.17E+02
C	19.5	1.46E+02
Be	28.5	1.71E+02

Table 1: Thicknesses that maximize the transmitted neutrons/proton ratio, at the end of each target, for different materials.

3.2. Neutron spectra analysis and material selection

Because it was found that the transmitted neutron spectra of the heavy targets are similar, to choose between the heavy targets their properties must compared. The use of bismuth and lead is not recommended because both have relatively low melting points (271.5^oC and 327^oC, respectively). Apart from the low melting points, lead is a toxic metal and bismuth produces ^{210}Po, through the reaction $^{209}Bi + n \rightarrow^{210} Bi \rightarrow^{210} Po + e^- + \bar{\nu}$, which is also toxic. Both tungsten and tantalum have high melting points (3422^oC and 3017^oC, respectively) and are less toxic than bismuth and lead. Table 1 shows that the transmitted neutrons/proton ratio is slightly higher for tantalum and it was found that its transmitted neutrons intensity is also slightly higher. However, since there were no experimental proton cross sections in MCNPX for tantalum, contrary to tungsten, the obtained results are dependent of a theoretical model and possibly less accurate. This makes tungsten to be the better candidate to be used as a target.

Even though the light targets are not going to be used, they should be compared to the heavy ones. The best light target, due to the characteristics of the transmitted neutron beam and due to its properties was chosen to be beryllium. Therefore, in figure 1 there is a comparison between the transmitted neutron spectra of a tungsten and beryllium targets, where it can be seen that the intensity of the transmitted neutrons, for $E > 50$ MeV, is higher in beryllium.

Since the damage induced by neutrons in materials is strongly non-linear [8], the presence of very fast neutrons is undesirable as they severely damage the samples being irradiated for research purposes. The highest neutron energies encountered in research environments are found in fusion reactors, in which the maximum neutron energy is approximately 15 MeV and is due to the fusion reaction $^2H +^3 H \rightarrow^4 He + n$, which releases a neutron with an energy of around 14 MeV. This means that, at the fast irradiation position, the neutron spectrum
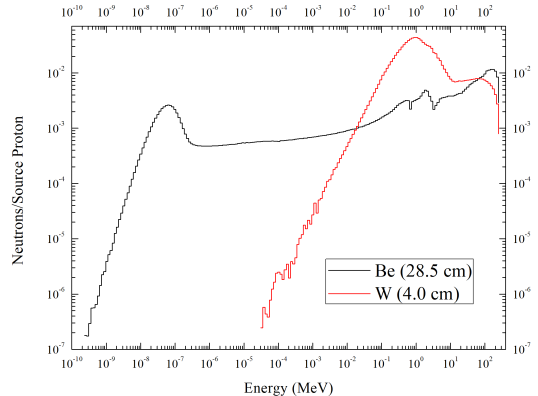

Figure 1: Comparison between the transmitted neutron spectra of the tungsten and beryllium targets.

should be rich in neutrons in the 1 - 15 MeV energy range and the neutron intensities in the 15 - 250 MeV energy range should be kept as low as possible. Since the intensity of the transmitted neutrons, for $E > 50$ MeV, is higher in beryllium, it could never be used as a target's material.

3.3. Alloy choice and beam analysis

Pure tungsten is an extremely hard metal and it is difficult to handle and machine, making it not suited to be used as the target's material. So, to solve these problems, a tungsten alloy must be used. Since kenertium is the most used tungsten alloy, a general purpose kenertium alloy was chosen as the target's material. Since the density of Kenertium is lower than the one of pure tungsten, the optimum target thickness was found to be 0.3 cm higher than the one of tungsten (or 4.3 cm), with the transmitted neutrons intensity and neutrons/protons ratio being approximately the same (table 2).

Materials	Neutrons/Source Proton	Neutrons/Proton
Kenertium	9.70E-01	1.63E+03
W	1.03E+00	1.96E+03

Table 2: Transmitted neutrons intensity and neutrons/protons ratio of the kenertium and tungsten targets.

Cyclotrons used for therapy can have proton beam intensities up to 5.0E12 protons/s in the case of the Varian/ACCEL 250 MeV proton cyclotron and to 1.9E12 protons/s in the case of the SHI 230 MeV proton cyclotron [12]. Using table 2, transmitted neutron intensities of approximately 4.8E12 and 1.8E12 neutrons/s can be achieved for a kenertium target, if the Varian/ACCEL or the SHI proton cyclotrons are used, respectively. The transmitted neutron intensity obtained with the Varian/ACCEL

cyclotron is approximately equal to the neutron intensity obtained with about 2 g of ^{252}Cf (yield: 2.4×10^{12} neutrons/g.s ; $t_{1/2} = 2.6y$). Since a ^{252}Cf neutron source costs 60 \$ per μg (cost in 1999 [4]), 2 g of ^{252}Cf would cost 120 M\$, which is higher than the cost of the cyclotron itself.

4. Characterization and optimization of the irradiation apparatus

Besides the target, discussed in the previous chapter, the irradiation apparatus includes (see figure 2): (i) a radiation trap, to reduce the leakage of neutrons through the entrance hole; (ii) a moderator, to decrease the energy of the fast neutrons released from the target; (iii) a target and moderator casing, to reduce neutron leakage; (iv) biological shielding, to decrease the radiation dose rates in the vicinity of the irradiation apparatus. It is desirable to have a fast neutron irradiation position - a position within the irradiation apparatus, where the neutron beam is rich in neutrons in the 1 - 15 MeV energy range - plus a thermal neutron irradiation position - a position where the neutron beam is rich in neutrons below 0.5 eV.

It was shown in chapter 3.2 that the neutrons produced in the kenertium target have energies well above the thermal range (figure 1), so if a thermal irradiation position is desired, the high energy neutrons released from the target must be moderated. However, placing the moderator immediately after the target could make impossible to set a fast irradiation position, due to the presence of a large number of thermal neutron immediately after the target. Therefore, two different configurations for the irradiation apparatus were studied (see figure 2), where the moderator (4 in the figure) was placed immediately after the target (A) and after a block of stainless steel (B).
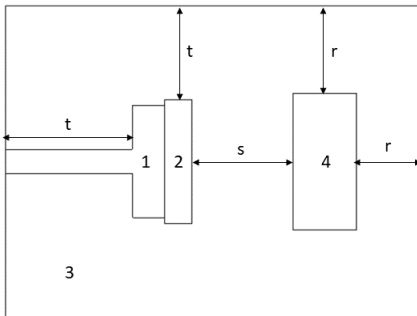

Figure 2: Schematic of the irradiation apparatus: 1 - Entrance hole and radiation trap; 2 - Kenertium target; 3 - Stainless steel casing; 4 - Moderator. Configuration A ($s = 0$ cm): $t = 40$ cm and $r = 39$ cm; Configuration B ($s = 45$ cm): $t = 30$ cm and $r = 20$ cm. Note: the picture is not to scale.

4.1. Configuration A: placing the moderator immediately after the target

The casing of the irradiation apparatus has to fulfil two requirements: it needs to decrease the leakage of neutrons by capture or scattering and, since some neutrons will manage to escape, the casing needs to be able to reduce the energy of a part of the fast ($E > 1$ MeV) neutrons because of their significant contribution to the radiation dose. It should also have good γ radiation shielding properties because of the γ production through (n, γ) reactions which occur throughout the irradiation apparatus. Iron (Fe) is a dense material made of heavy nuclei (55.84 g/mol), making it good at impeding neutron leakage by scattering and at shielding γ radiation. Additionally, one can take advantage of its neutron inelastic scattering cross section to reduce the energy of a part of the fast neutrons. To avoid corrosion problems stainless steel was selected instead of pure iron.

Since it is impossible to know, before characterizing the whole irradiation apparatus, if a particular side wall thickness t is effective at decreasing neutron leakage by scattering, it was chosen, as a first reasonable guess, a value of $t = 40$ cm. The entrance hole has a cross-section area of 4x4 cm^2, deemed a reasonable value because the incident proton beam used in the simulations had a width of 2 cm [13]. The radiation trap has a cross-section area of 18x18 cm^2, which seemed reasonable enough to reduce the leakage of neutrons through the casing. Since the cross-section area of the moderator was set to have 22x22 cm^2 and the target has 20x20 cm^2, then one has $r = 39$ cm as an initial estimate.

In a nuclear reactor either reactor grade graphite (Carbon, C) or water (H_2O) are used as moderators. Since it would be complicated to use water in the apparatus, polyethylene (C_2H_4) is a good alternative as it has hydrogen atoms in its composition. Therefore, reactor grade graphite and polyethylene were investigated as potential moderators. The richness of a neutron beam in thermal neutrons can be evaluated by calculating the $\frac{0-0.5eV}{0-250MeV}$ neutron ratio. In tables 3 and 4 it can be seen that the moderator lengths that maximize the transmitted $\frac{0-0.5eV}{0-250MeV}$ neutron ratio are 10 cm and 60 cm, for polyethylene and graphite respectively. To irradiate samples, irradiation cavities inside the moderator must be made, however they will increase the moderator length needed to thermalize the neutron beam produced in the target. Also, the thermal irradiation of a sample benefits massively from having a stream of backscattered thermal neutrons. So, it was chosen that, for both moderators, their length should be set equal to the double of the length needed to maximize the transmitted $\frac{0-0.5eV}{0-250MeV}$ neutron ratio. Therefore moderator lengths of 20 cm and

120 cm were chosen for polyethylene and graphite, respectively.

Length (cm)	$\frac{0-0.5eV}{0-250MeV}$
6	2.86E-01
8	3.28E-01
10	3.29E-01
12	3.04E-01
14	2.70E-01

Table 3: Values of the transmitted $\frac{0-0.5eV}{0-250MeV}$ neutron ratio, taken at the end of a polyethylene moderator, for several lengths.

Length (cm)	$\frac{0-0.5eV}{0-250MeV}$
40	8.34E-02
50	1.01E-01
60	1.03E-01
70	9.60E-02
80	8.66E-02

Table 4: Values of the transmitted $\frac{0-0.5eV}{0-250MeV}$ neutron ratio, taken at the end of a reactor grade graphite moderator, for several lengths.

It was stated, in the beginning of this chapter, that setting a fast neutron irradiation position using this configuration (A) for the irradiation apparatus could be an impossible task due to the presence of a large number of thermal neutron immediately after the target. Table 5 shows the $\frac{1-15MeV}{0-0.5eV}$ neutron ratio, at the fast irradiation positions (set immediately after the target, for both moderators, in order to reduce neutron moderation) of a 20 cm and 120 cm in length polyethylene and reactor grade graphite moderators, respectively. It shows that the thermal neutron intensity is, at best, only one order of magnitude lower than the intensity of the neutrons in the 1 - 15 MeV energy range, confirming that configuration A cannot be used for the irradiation apparatus, due to the impossibility of setting a fast irradiation position.

Moderator	$\frac{1-15MeV}{0-0.5eV}$
Polyethylene (20 cm)	1.59
Graphite (120 cm)	5.23E+01

Table 5: Values of the $\frac{1-15MeV}{0-0.5eV}$ neutron ratios, taken at the fast irradiation positions (set immediately after the target) for a 20 cm and 120 cm in length polyethylene and reactor grade graphite moderators, respectively.

Even though configuration A cannot be used for setting a fast neutron irradiation position, a possible thermal neutron irradiation position should still be studied, because it will further justify the use of configuration B for the irradiation apparatus, as well as give insight on the length and material of its moderator. The thermal irradiation positions can be established by finding the maximum value of the $\frac{0-0.5eV}{0-250MeV}$ neutron ratio along the polyethylene and reactor grade graphite moderators. Therefore, these positions were found to be located at 8.5 cm and 55 cm from the target, for polyethylene and graphite, respectively. The values of the $\frac{0-0.5eV}{0-250MeV}$ and the $\frac{0-0.5eV}{1-250MeV}$ neutron ratios, for both moderators, at the respective thermal irradiation positions, are presented in table 6. The fast neutron intensity ($E > 1$ MeV) should be as low as possible, or else the purpose of an irradiation position of this type is lost. Since the thermal neutron intensities are approximately of the same order of magnitude as those of the fast neutrons, this configuration (A) is not suited for setting a thermal irradiation position.

Moderator	$\frac{0-0.5eV}{0-250MeV}$	$\frac{0-0.5eV}{1-250MeV}$
Polyethylene (20 cm)	6.59E-01	4.01
Graphite (120 cm)	1.50E-01	1.65

Table 6: Values of the $\frac{0-0.5eV}{0-250MeV}$ and the $\frac{0-0.5eV}{1-250MeV}$ neutron ratios, at the thermal irradiation positions, for the 20 cm and 120 cm in length polyethylene and reactor grade graphite moderators, respectively.

4.2. Configuration B: placing the moderator after a stainless steel block

Configuration B differs from configuration A by having a block of stainless steel between the target and the moderator. It will provide a mean for setting a fast irradiation position, since neutron moderation in stainless steel (Fe), for neutrons with $E < 1$ MeV, is low. Also, having a stainless steel block between the target and the moderator will allow for the fast irradiation position to be located far enough from the moderator and from the backscattered thermal neutrons produced in it. The energy of a part of the fast ($E > 1$ MeV) neutrons, produced in the target, will also be reduced by taking advantage of the neutron inelastic scattering of iron (Fe), reducing the intensity of the fast neutrons at the thermal irradiation position. The dimensions of the irradiation apparatus for configuration B are the same as those used in configuration A, apart from: t, which was changed to 30 cm, since it was found to be enough to contain most of the neutron beam, as it travels through the stainless steel block; r, which was changed to 20 cm, since the cross-section area of the moderator was changed to 40x40 cm^2 to allow samples of different sizes and shapes to be placed inside it for irradiation purposes.

To determine an adequate length (s) from the kenertium target to the moderator, the transmit-

ted $\frac{1-250MeV}{0-250MeV}$ neutron ratio, taken at the beginning of the moderator, should be minimized. Since it was discovered that the moderator produces a large number of backscattered neutrons, the moderator in figure 2 was removed, so that this ratio could be properly evaluated at the end of the stainless block. The transmitted $\frac{1-250MeV}{0-250MeV}$ neutron ratio, as a function of s, is presented in figure 3 and, to keep the dimensions of the irradiation apparatus reasonably low, it was decided that the transmitted $\frac{1-250MeV}{0-250MeV}$ neutron ratio should have a maximum value of 0.1. However, to irradiate samples inside the stainless steel block, cavities must be made in it, which will increase the stainless steel length needed to reduce the energy of a part of the neutrons with $E > 1$ MeV, produced in the target. Therefore, to take it in consideration, the most appropriate length from the kenertium target to the moderator was found to be $s = 45\ cm$.
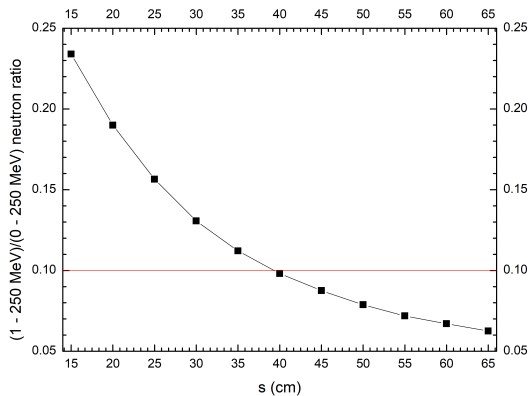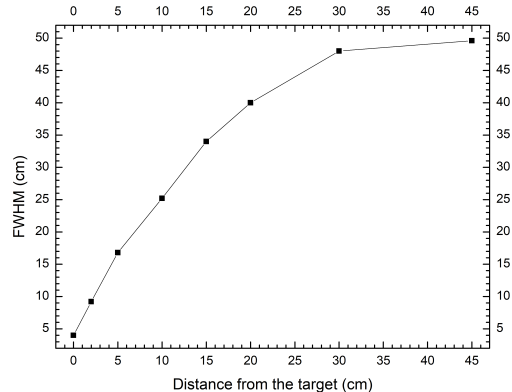

Figure 4: Full widths at half maximum (FWHM) of the neutron beam, as a function of the distance to the target. Note: the line was drawn merely to guide the eye.

From table 6, it can be seen that using a polyethylene moderator would produce a slightly better thermal irradiation position, due to the marginally higher neutron ratios. Also, the length of the polyethylene moderator to produce such results is much smaller than the length of the graphite, which reduces the cost of the irradiation apparatus. For these reasons, a polyethylene moderator will be used for configuration B. Concerning its length, it was found that a 20 cm polyethylene moderator would be enough to thermalize the neutron beam produced in the target. This means that surely the same length will be enough to thermalize the neutron beam in configuration B, since the energy of a part of the fast ($E > 1$ MeV) neutrons, produced in the target, has already been reduced by the time they enter the moderator. Using the same method used in configuration A, the thermal irradiation position of configuration B was found to be located at 7.5 cm from the beginning of the polyethylene moderator and the values of the $\frac{0-0.5eV}{0-250MeV}$ and $\frac{0-0.5eV}{1-250MeV}$ neutron ratios, at this irradiation position, are presented in table 7.

Figure 3: Values of the transmitted $\frac{1-250MeV}{0-250MeV}$ neutron ratio, taken at the end of the stainless block, as a function of s. Note: the black line was drawn merely to guide the eye.

Due to the inelastic scattering cross section of Fe, one might think that the fast irradiation position should be set as close as possible to the target. However, for properly setting a fast irradiation position, the broadening of the neutron beam, as it travels through stainless steel, must also be considered. For properly irradiate a sample, the neutron fluences should be kept as homogeneous as possible across the sample's surfaces. However, since regions with homogeneous neutron fluences in stainless steel are not possible, it was chosen that the neutron fluences, across a sample's surface, should never be lower than 50% of their maximum value. Remembering that the neutron beam is symmetric in the Y-Z directions, the region in space, for a given distance from the target, where the neutron fluences are above 50% of it's maximum value, is a circle, centred around the X axis, with a diameter equal to the full width at half maximum of the neutron beam. The full widths at half maximum (FWHM) of the neutron beam, as a function of the distance to the target, are presented in figure 4.

Moderator	$\frac{0-0.5eV}{0-250MeV}$	$\frac{0-0.5eV}{1-250MeV}$
Polyethylene (20 cm)	8.17E-01	1.89E+01

Table 7: Values of the $\frac{0-0.5eV}{0-250MeV}$ and the $\frac{0-0.5eV}{1MeV-250MeV}$ neutron ratios, at the thermal irradiation position, for the 20 cm in length polyethylene moderator.

In figure 5 the neutron beam profile, at the thermal irradiation position, is calculated and it can be seen that the neutron fluences remain practically constant across the polyethylene moderator, which is an excellent result because it allows a sample to be thermally irradiated with practically constant neutron fluences across its surface.
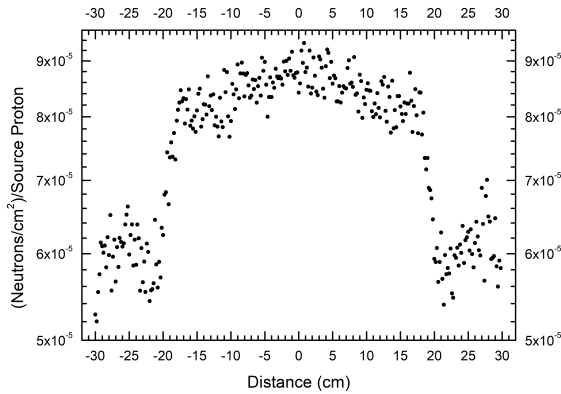
Figure 5: Neutron beam profile, taken at the intersection of a plane X, at the thermal irradiation position, with plane Z=0 as a function of y (or distance to the centre of the irradiation apparatus).

4.3. Comparison between the irradiation apparatus and the Portuguese Research Reactor (RPI)

To compare the neutron fluence rates obtained at the RPI with those obtained at the irradiation apparatus, a proton beam intensity must be chosen. An incident proton beam intensity of 5E12 protons/s was selected, which is the maximum intensity that the 250 MeV Varian/ACCEL proton cyclotron is able to attain. In table 8, the neutron fluence rates at the two irradiation positions of the irradiation apparatus (IA) are compared with "similar" positions that used to be available in the Portuguese Research Reactor (RPI): an in-pool irradiation position (position 54 of the core grid) and a dry irradiation chamber for irradiation with fast neutrons.

While the irradiation apparatus outperforms the RPI, for irradiations with fast neutrons, the same cannot be said for irradiations with thermal neutrons. Since the RPI is a 1 MW reactor, there are, approximately, 10^{16} neutrons/s available for irradiations. With table 2 and assuming that an incident proton beam with an intensity of 5E12 protons/s was utilized, the neutron intensity produced in the kenertium target is equal to 4.8E12 neutrons/s. Since the intensities in the RPI are almost 4 orders of magnitude higher when compared to those produced by the target, an irradiation position in the reactor core will always have much higher

Device (position)	Neutron fluence rate	
	0 - 0.5 eV	1 - 15 MeV
IA (fast)	3.3E+06	2.3E+09
RPI (irr. chamber)	2.3E+07	4.0E+08
IA (thermal)	3.7E+08	4.2E+06
RPI (54 in grid)	25.0E+12	25.6E+11

Table 8: Neutron fluence rates (neutrons/cm^2/s), for the 0 - 0.5 eV and 1 - 15 MeV energy ranges, obtained: at a fast (10 cm from the target) and thermal irradiation positions of the irradiation apparatus; at the in-pool irradiation position 54 and at the dry (outside the reactor pool) fast neutron irradiation chamber [7, 9] of the Portuguese Research Reactor (RPI).

neutron fluence rates than any irradiation position in the irradiation apparatus.

5. Shielding and activation

The main goal to be achieved with a biological shield surrounding the irradiation apparatus is to ensure that, in its vicinity, the radiation dose rate limit of 20 mSv over the course of a year, imposed by the Portuguese law, is not exceeded [1]. For calculating the dose rates, the neutron and γ fluences will be supplied by the MCNPX code which will then be converted into dose rates by using conversion factors (the factor for converting fluence to dose rate) that can be found in ICRP-21 [3]. Since the irradiation apparatus will be subjected to relatively high fluence rates of neutrons with different energies, CINDER'90 [14] code will be used to calculate the activity of its different components, as well as the main radionuclides produced.

5.1. Implementation of the biological shielding

Before implementing the biological shielding, there are some aspects that must be made clear. First, in the following dose rate calculations the radiation from the decay of the radioisotopes was not taken into account. Also, the contribution to the total radiation dose rate from the protons was not considered. Second, the thickness of the biological shield will be constant (figure 6) and was calculated in order to assure that the radiation dose rate limit is never exceeded. Finally, all of the dose rates were calculated immediately after the irradiation apparatus/biological shield, which means that a worker will be able to stand right next to it without exceeding the dose rate limits and that there will be no restricted zones to the personnel in the surroundings of the irradiation apparatus (apart from the zone behind the entrance hole).

The irradiation apparatus has the shape of a parallelepiped (figure 6) and so, six surfaces bound

it and are the following: one surface at the beginning of the irradiation apparatus (S1), where the entrance hole is localized; four side walls parallel to the symmetry axle (one of the four is S2); one surface at the end of the irradiation apparatus (S3). The incident proton beam needs to be focused into the kenertium target so, the entrance hole cannot be covered with a biological shield and, since there will be direct streaming of neutrons through the entrance hole, the zone behind surface S1 must be restricted to the personnel. Also, since the intensity of the neutron beam is higher along the centre (symmetry axle) of the irradiation apparatus, the highest dose rate across surface S3 is located at its centre.

in shielding against neutrons, due to the presence of H. To calculate the thickness of the biological shield, the dose rates that follow (figure 8) are calculated at the locations of the highest dose rate across surfaces S2 and S3 and assuming an incident proton beam with an intensity of 5E12 protons/s.

Figure 7: Total radiation dose rates across a line, parallel to the symmetry axle of the irradiation apparatus, that crosses the centre of the side wall S2, as a function of the distance of any point of that line to the surface S1.
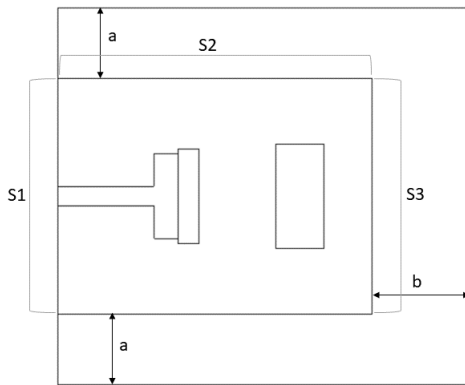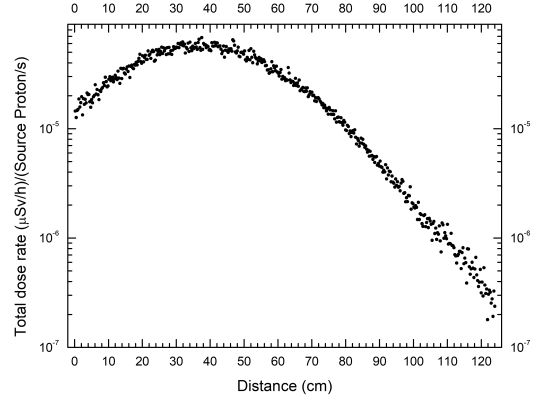

Figure 6: Irradiation apparatus with a barytes-limonite concrete biological shield surrounding it. Here, the surfaces of the irradiation apparatus where radiation leakage occurs are highlighted (S1, S2 and S3). The concrete's thickness to shield the side walls (a) and surface S3 (b) are also shown ($a = 3.0$ m and $b = 4.0$ m). Note: the picture is not to scale.

Since the regions in space where the neutron fluences are constant are circumferences and the irradiation apparatus has the shape of a parallelepiped, the highest dose rate across side wall S2 must be located somewhere across a line, parallel to the symmetry axle of the irradiation apparatus, that crosses the centre of S2. The total radiation dose rates, throughout the mentioned line, as a function of the distance of any point of that line to the surface S1, are presented in figure 7, where it can be seen that the maximum dose rate is located at 37.54 cm from the surface S1.

Since both neutrons and γ radiation need to be shielded, concrete was chosen as the biological shield's material and, to decrease its dimensions, a heavy concrete containing both baryte and limonite aggregates will be used. Because limonite is an hydrated iron ore, a heavy concrete with a limonite aggregate presents a particularly good performance
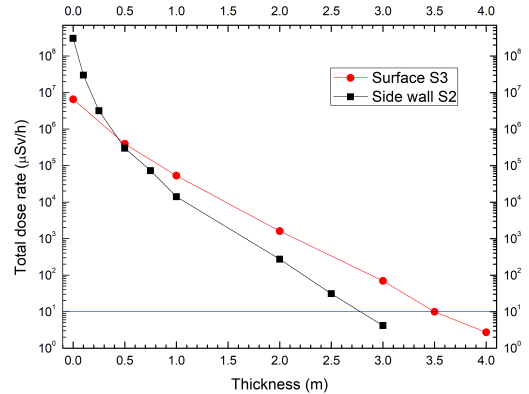

Figure 8: Total radiation dose rate values, as a function of the thickness of the barytes-limonite concrete biological shield. Note: the black and red lines were drawn merely to guide the eye.

Generally speaking, the personnel only works 50 weeks per year (4 weeks of holidays), 5 days per week (2 days of weekend) and 8 hours per day, which means that a dose rate of 10 μSv/h should not be exceeded. Figure 8 presents the total radiation dose rates, as a function of the shield's thickness, for the side wall S2 and surface S3. As it can be seen, a thickness of $a = 3.0$ m and $b = 4.0$ m are required

to assure that the dose rate limit is not exceeded for side wall S2 and surface S3, respectively.

5.2. Activation of the irradiation apparatus

The irradiation apparatus will be subjected to relatively high fluence rates of neutrons with different energies, implying that there will be activation of its various components, which will be dependent on the neutron fluence rates, energies and the composition of the materials of the components. Therefore, to calculate the activation of the irradiation apparatus using the CINDER'90 code [14], it must be divided into different cells (or volumes) as shown in figure 9.
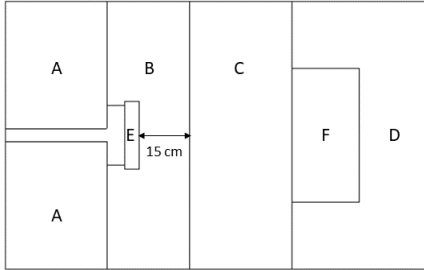

Figure 9: Division of the irradiation apparatus in different cells (or volumes), for the purpose of calculating their activity and produced radionuclides. Note: the picture is not to scale.

The activity and radionuclides produced in each cell are heavily dependent on the amount of time that the irradiation apparatus is operating and on the intensity of the incident proton beam. Therefore it was chosen that CINDER'90 code would be used to simulate a continuous operation of 120 h of the irradiation apparatus, with an incident proton beam with an intensity of 1E12 protons/s. The total activity and main radionuclides produced were evaluated immediately, 1 day and 30 days after the shutdown of the cyclotron and are presented in tables 9 to 12.

Cell	Activity (Ci/cm^3)		
	Shutdown	1 day	30 days
A	8.22E-06	2.98E-07	1.18E-07
B	1.45E-05	6.44E-07	2.48E-07
C	6.27E-06	2.11E-07	9.14E-08
D	4.42E-07	2.03E-08	9.24E-09
E	2.37E-03	5.26E-04	4.35E-05
F	6.31E-08	5.50E-12	5.48E-12

Table 9: Total activity of each different cell, evaluated immediately, 1 day and 30 days after the shutdown of the cyclotron.

As expected, the radionuclides with shorter half-lives are dominant when the time span after the

Cell	Main radionuclides		
	1	2	3
A	^{56}Mn	^{58m}Co	^{51}Cr
B	^{56}Mn	^{58m}Co	^{51}Cr
C	^{56}Mn	^{58m}Co	^{51}Cr
D	^{56}Mn	^{51}Cr	^{58m}Co
E	^{183m}W	^{187}W	^{58m}Co
F	^{8}Be	^{12}B	^{11}C

Table 10: Radionuclides with the higher activities immediately after the shutdown of the cyclotron, for each different cell.

Cell	Main radionuclides		
	1	2	3
A	^{51}Cr	^{58m}Co	^{58}Co
B	^{51}Cr	^{58m}Co	^{58}Co
C	^{51}Cr	^{58m}Co	^{58}Co
D	^{51}Cr	^{58m}Co	^{56}Mn
E	^{187}W	^{185}W	^{58m}Co
F	^{3}H	^{14}C	^{10}Be

Table 11: Radionuclides with the higher activities 1 day after the shutdown of the cyclotron, for each different cell.

Cell	Main radionuclides		
	1	2	3
A	^{51}Cr	^{58}Co	^{55}Fe
B	^{51}Cr	^{58}Co	^{55}Fe
C	^{51}Cr	^{58}Co	^{55}Fe
D	^{51}Cr	^{55}Fe	^{58}Co
E	^{185}W	^{181}W	^{58}Co
F	^{3}H	^{14}C	^{10}Be

Table 12: Radionuclides with the higher activities 30 days after the shutdown of the cyclotron, for each different cell.

shutdown of the cyclotron is short, whereas the radionuclides with longer half-lives are dominant when the time span after the shutdown of the cyclotron is long.

6. Conclusions

In this work the viability of producing neutrons using a 250 MeV proton cyclotron coupled to a target was studied. This cyclotron was considered as a source of protons for irradiation of a neutron producing target, as the installation of a 250 MeV proton cyclotron for radiation therapy in the Loures Campus (CTN) of IST is foreseen in the near future. It was found that a kenertium (tungsten alloy) target is the most appropriate for producing a neutron beam with the required characteristics and, using an incident proton beam with an intensity of 5.0E12 protons/s, it produces a transmitted neu-

tron beam with an intensity approximately equal to what would be obtained with 2 g of ^{252}Cf, which has a cost much higher than the cyclotron itself.

For the purpose of implementing irradiation positions with spectra rich in fast and thermal neutrons, it was found that placing the neutron moderator immediately after the target would make impossible setting a fast irradiation position. Therefore, another configuration for the irradiation apparatus was studied, in which there is a stainless steel block between the target and the moderator. This configuration (B) made possible the setting of the two irradiation positions and it was found that the fast one was able to outperform a "similar" position that used to be available at the RPI. Regarding the irradiations with thermal neutrons, it was found that the irradiation apparatus is not capable of outperforming the RPI, since this type of irradiations are performed close to the reactor core. Finally, to ensure that the radiation dose rate limit of 20 mSv over the course of a year is not exceeded, the irradiation apparatus was properly shielded and, since it will be subjected to relatively high fluence rates of neutrons, the activation and radionuclides produced in its components were calculated using the CINDER'90 code.

In the future some additional improvements can be made to this work, such as: studying tantalum as a possible target material; formulating the full width at half maximum of the neutron beam as a function of the distance to the target; performing simulation "runs" for sensitivity studies on variations of the dimension parameters of the components of the irradiation apparatus; optimizing the biological shield of the irradiation apparatus.

References

[1] Decreto-Lei, n108/2018, 3 December.

[2] Resolução do conselho de ministros n° 28/2018. Diário da República, 9 March. 1st series, n° 49.

[3] *Data for Protection Against Ionizing Radiation from External Sources: Supplement to ICRP Publication 15*. Number 21 in ICRP Publications. Pergamon Press, Oxford, 1973.

[4] P. Balo, J. Knauer, and R. Martin. Production, distribution, and applications of Californium-252 neutron sources. 1999.

[5] H. W. Bertini. Low-energy intranuclear cascade calculation. *Phys. Rev.*, 131:1801–1821, 1963.

[6] H. W. Bertini. Secondary particle spectra from the interaction of 30- to 340- MeV protons on complex nuclei: Experimental data and comparison with theory. *Phys. Rev.*, 162:976–982, 1967.

[7] A. Fernandes, J. Santos, J. Marques, A. Kling, A. Ramos, and N. Barradas. Validation of the Monte Carlo model supporting core conversion of the Portuguese Research Reactor (RPI) for neutron fluence rate determination. *Annals of Nuclear Energy*, 37:1139, 2010.

[8] M. Huhtinen and P. Aarnio. Pion induced displacement damage in silicon devices. *Nuclear Instruments and Methods in Physics Research Section A: Accelerators, Spectrometers, Detectors and Associated Equipment*, 335:580–582, 1993.

[9] J. Marques, A. Ramos, A. Fernandes, and J. Santos. Irradiation of electronic components and circuits at the Portuguese Research Reactor: Lessons learned. *IEEE Transactions on Nuclear Science*, 63:1485–1490, 2016.

[10] G. Mckinney. MCNPX user's manual, version 2.6.0, 2008.

[11] R. Serber. Nuclear reactions at high energies. *Phys. Rev.*, 72:1114–1115, 1947.

[12] V. Smirnov and S. Vorozhtsov. Modern compact accelerators of cyclotron type for medical applications. *Physics of Particles and Nuclei*, 47:863–883, 2016.

[13] F. Tommasino, M. Rovituso, S. Fabiano, S. Piffe, C. Manea, S. Lorentini, S. Lanzone, Z. Wang, M. Pasini, W. Burger, C. La Tessa, E. Scifoni, M. Schwarz, and M. Durante. Proton beam characterization in the experimental room of the trento proton therapy facility. *Nuclear Instruments and Methods in Physics Research A*, 869:15–20, 2017.

[14] W. Wilson, S. Cowell, T. England, A. Hayes, and P. Moller. A manual for CINDER'90 version 07.4 codes and data LA-UR-07-8412. Technical report, Los Alamos National Laboratory, 2008. Version 07.4.2.